View Online
Dynamic Article Links

Journal of
Materials Chemistry

Cite this: *J. Mater. Chem.*, 2011, **21**, 7714

www.rsc.org/materials

PAPER

Pyrazino[2,3-g]quinoxaline-based conjugated copolymers with indolocarbazole coplanar moieties designed for efficient photovoltaic applications†

Qiang Peng,*[a] Xiangju Liu,[a] Yuancheng Qin,[a] Jun Xu,[a] Mingjun Li[a] and Liming Dai*[b]

Received 28th January 2011, Accepted 20th March 2011
DOI: 10.1039/c1jm10433k

A series of low band gap copolymers consisting of electron-accepting pyrazino[2,3-g]quinoxaline (PQx) and an electron-donating indolo[3,2-b]carbazole and thiophene units have been designed and synthesized by Stille coupling polymerization. Their optical and electrical properties could also be facilely fine-modulated for photovoltaic application by adjusting the donor/acceptor ratios. UV-vis measurements showed that increasing the content of PQx units led to enhanced absorption. The band gaps obtained from UV-vis spectra, CV scanning, and DFT modeling all indicated a narrowing band gap with increasing the PQx content in the copolymer structure. The photovoltaic solar cells (PSCs) based on these copolymers were fabricated and tested with a structure of ITO/PEDOT:PSS/copolymer:PCBM/Ca/Al under the illumination of AM 1.5G, 100 mW cm^{-12}. The best performance was achieved using **P3**/[70]PCBM blend (1 : 3) with $J_{sc} = 9.55$ mA cm^{-2}, $V_{oc} = 0.81$ V, FF = 0.42, and PCE = 3.24%, which is the highest efficiency for the PQx and indolo[3,2-b]carbazole based devices. The present results also indicate that the efficient photovoltaic materials with suitable electronic and optical properties can be achieved by just fine-tuning the ratios of the strong electron-deficient accepters and large-π planar donors.

Introduction

The sunlight is a clean, abundant and virtually limitless energy source which can be used to address the growing global energy needs. Recently, polymer photovoltaic cells (PVCs) have received much attention because of their flexibility, facile processibility, low weight and low production cost.[1–5] Since the 1990s, poly-(p-phenylene vinylene)s (PPVs) and the polythiophenes (PTs) were most studied conjugated polymers with high power conversion efficiencies (PCE).[6,7] However, their relatively large bandgaps limited the short circuit current (J_{sc}), reducing the PCE. In order to further improve the efficiency, low band gap conjugated polymers were developed to better match the solar spectrum and thereby produce higher J_{sc}.[8,9] Great progress has been made in PVCs based on bulk-heterojunction (BHJ) networks made of low band gap conjugated polymers and fullerene derivatives in the past few years, and efficiency as high as more than 7% has been reported.[10,11]

In general, the power conversion efficiency (PCE) relies on the open-circuit voltage (V_{oc}), the short-circuit current density (J_{sc}), and the fill factor (FF) of the devices. In PVCs, J_{sc} is controlled by the matchment between the absorption of the conjugated polymers and the solar spectrum.[12] The V_{oc} is determined by the difference between the energy levels of lowest unoccupied molecular orbital (LUMO) of the fullerene derivatives (as electron acceptor, A) and the highest occupied molecular orbital (HOMO) of conjugated polymers (as electron donor, D).[13] Therefore, further improvement in the PCE demands the development of novel conjugated polymers with appropriate energy levels and broader absorption with the solar spectrum. On the other hand, the high charge carrier mobility of polymer semiconductors should also be taken into account.[14]

The powerful strategy to achieve a low band gap conjugated polymer is to incorporate alternating donor (D) and acceptor (A) moieties segments in the polymer main-chain. Base on this type of push-pull structure, efficient photoinduced intramolecular charge transfer (ICT) can easily take place from the donor to the acceptor upon photoexcitation and generate an absorption band at the lower energy.[15] Very recently, series of conjugated polymers containing quinoxaline (Qx) derivatives were reported for the production of low band gap conjugated polymers for efficient PVCs.[16–20] Qx heterocycles were chosen as electron-acceptor segments in these work because of their high electron affinity attributed to symmetric unsaturated imine nitrogen (C=N)

[a]*School of Environmental and Chemical Engineering, Nanchang Hangkong University, Nanchang, 330063, P. R. China. E-mail: qiangpengjohnny@yahoo.com; Fax: +86-0791-3953369; Tel: +86-0791-3953369*
[b]*Department of Chemical Engineering, Case Western Reserve University, Cleveland, Ohio, 44106*
† Electronic supplementary information (ESI) available. See DOI: 10.1039/c1jm10433k

structures.[15] In comparison with Qx, the pyrazino[2,3-g]quinoxaline (PQx) unit is relatively more electron-deficient and more rigid. Therefore, replacing Qx units in conjugated polymers with PQx moieties can give rise to the corresponding polymers with lower band gap, higher ionization potential (IP) and more rigid structures. Up to now, only a few molecular or polymeric materials based on PQx were explored for PVCs.[21,22] In addition, the introduction of a planar π–π system in the polymer backbone allows the polymer to form long-range intermolecular π–π stacking arrangements, which can lead to a high charge carrier mobility. Therefore, a new series of copolymers consisting of an electron-accepting pyrazino[2,3-g]quinoxaline (PQx) and an electron-donating coplanar indolo[3,2-b]carbazole and thiophene units have been designed (Scheme 1). Recently, Krebs and co-workers studied the stability of carbazole units and generally found the N-alkyl bond as a weak point in air.[23,24] However, indolo[3,2-b]carbazole derivatives showed relatively high hole mobilities of more than 0.02 $cm^2\ V^{-1}\ s^{-1}$ in organic field-effect transistors (OFETs).[25,26] Also, low band gap conjugated copolymers of indolo[3,2-*b*]carbazole with benzothiadiazole (BT) exhibited the high power conversion efficiency in PVCs.[27,28] So, it is reasonable to expect that these polymers would have narrower band gaps and higher charge mobility. Their optical and electrical properties also can be facilely fine-modulated by adjusting the donor/acceptor ratios.[29,30]

Results and discussion

Synthesis and characterization

The synthetic route of the monomers and copolymers is outlined in Scheme 1. Bromination of 2,1,3-benzothiadiazole with Br_2 and HBr (47%) gave 4,7-dibromo-2,1,3-benzothiadiazole (**1**),[28] which was subsequently nitrificated a 1 : 1 (vol/vol) of fuming nitric acid and fuming sulphuric acid to afford 4,7-dibromo-5,6-dinitro-2,1,3-benzothiadiazole (**2**) in 28% yield after recrystallization in ethanol.[31] The Stille coupling reaction between compound **2** and 5-tri-*n*-butylstannyl-3-*n*-hexylthiophene in the presence of $PdCl_2(PPh_3)_2$ afforded 4,7-di-(3-*n*-hexylthiophen-2-yl)-5,6-dinitro-2,1,3-benzothiadiazole (**3**) in 77% yield. 2,3,7,8-Tetraethyl-5,10-di-(3-*n*-hexylthiophen-2-yl)-pyrazino[2,3-*g*]-quinoxaline (**4**) was then synthesized in 56% yield using a one-pot reaction. **3** was first reduced to its corresponding diamine by heating at 60 °C in acetic acid with a excess of zinc powder without separation. After 1.5 h, 3,4-hexanedione was added to above reactant solution and condensed with the diamine derivative to yield **4**. Monomer **5** was finally prepared by dibromination of **5** with N-bromosuccinimide (NBS) in a 1 : 1 (vol/vol) mixture of acetic acid and chloroform in 79% yield. 3,9-Dibromo-6-hexyl-5,11-dihydroindolo[3,2-*b*]carbazole (**6**) was synthesized in one-pot method by the reaction of 5-bromoindole with *n*-heptaldehyde using iodine as a catalyst and subsequently

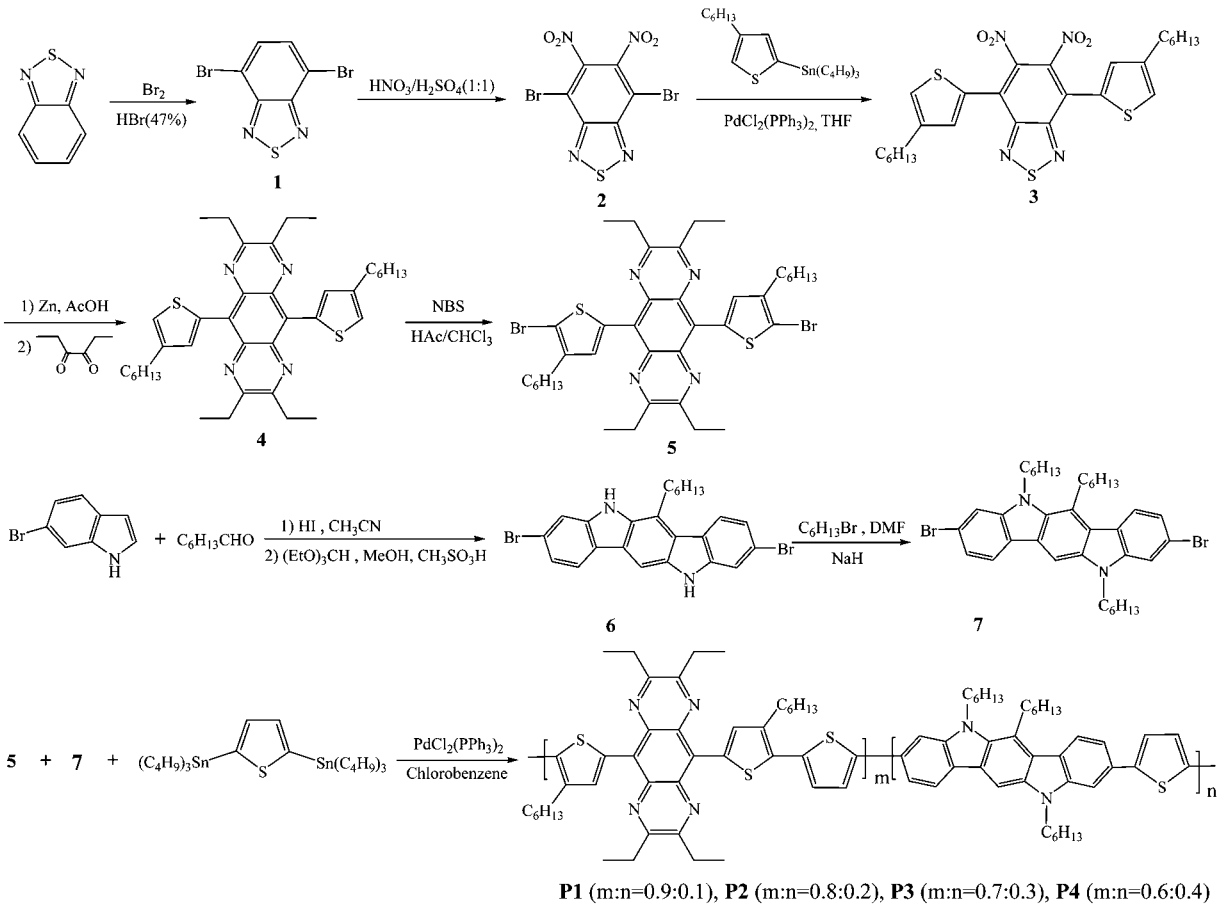

P1 (m:n=0.9:0.1), **P2** (m:n=0.8:0.2), **P3** (m:n=0.7:0.3), **P4** (m:n=0.6:0.4)

Scheme 1 Synthetic route for monomers and random conjugated copolymers.

treated with triethyl orthoformate in methanol in the prescence of a catalyst amount of methanesulfonic.[32] The N-hexylation reaction of **6** was carried out in a DMF solution with *n*-bromohexane using sodium hydride as an alkali, which was used to give a high solubility to the monomer **7** containing indolo[3,2-*b*]carbazole segment. Random copolymers **P1–P4** that consist of indolo[3,2-*b*]carbazole and thiophene as electron-donating units and pyrazino[2,3-g]quinoxaline (PQx) as electron-accepting moieties were synthesized by Pd(0)-catalyzed Stille coupling polymerization in chlorobenzene, where the monomer **5** reacted with 2,5-bis(tributylstannyl) thiophene and **7** at different molar ratios (see Experimental). The structures of the copolymers were confirmed with NMR spectroscopy and elemental analysis.

All of the copolymers show good solubility at room temperature in organic solvents such as chloroform, tetrahydrofuran, toluene, xylene and chlorobenzene. The incorporation of hexyl or ethyl side chains on indolo[3,2-*b*]carbazole, thiophene and PQx segments enables them to have a good solubility. The weight-average molecular weight (M_w) and polydispersity index (M_w/M_n) were measured by gel permeation chromatography (GPC) using THF as the eluent and polystyrenes as the internal standards. The results showed that **P1–P4** have a M_n of 7200–8500 with polydispersity indices of 1.76–1.98 (Table 1). Moreover, the resulting copolymers exhibited a good thermal stability with decomposition onset temperatures (T_d) (about 5% weight-loss) of 290–343 °C as measured by thermogravimetric analysis (TGA). The glass transition temperatures (T_g) of these copolymers were also investigated by differential scanning calorimetry (DSC), and the glass transition temperatures were determined to be 72–90 °C, respectively. The combinations of such good thermal properties are adequately suitable for PVCs and other optoelectronic devices.

Optical properties

All electronic absorption properties of the obtained copolymers were measured both in THF solutions (Fig. 1a) and thin films on quartz slides (Fig. 1b). The spectroscopic data are also listed in Table 2. As shown in Fig. 1a, all absorption spectra of these copolymers in THF solutions have one broad distinct peak in the wavelength range of 450–1000 nm, arising from the n–π* transition from PQx heterocyclic units, which redshifted with the increase of PQx content. This indicated that better absorbance could be achieved with incorporation of more PQx units. Another peak attributed to π–π* electronic transitions of the conjugated polymer backbones were also observed in the wavelength range of 350–450 nm. This absorbance as well as the identical absorption from benzic cycle (*ca.* 300 nm) enhanced from **P1** to **P4** indicating the increasing the content of indolo[3,2-*b*]carbazole moieties in the polymer chains, which agreed with the molar ratios (see Experimental).

Table 1 Molecular weights and thermal properties of the copolymers

Copolymers	Yield (%)	M_n[a] (× 10^3)	PDI[a] (M_w/M_n)	T_d[b] (°C)	T_g[c] (°C)
P1	58	7.6	1.85	320	72
P2	60	8.0	1.92	343	75
P3	61	8.5	1.98	305	77
P4	63	7.9	1.86	301	85

[a] Molecular weights and polydispersity indices were determined by GPC in THF using polystyrene as standards. [b] Onset decomposition temperature measured by TGA under N_2. [c] Glass transition temperature measured by DSC under N_2.

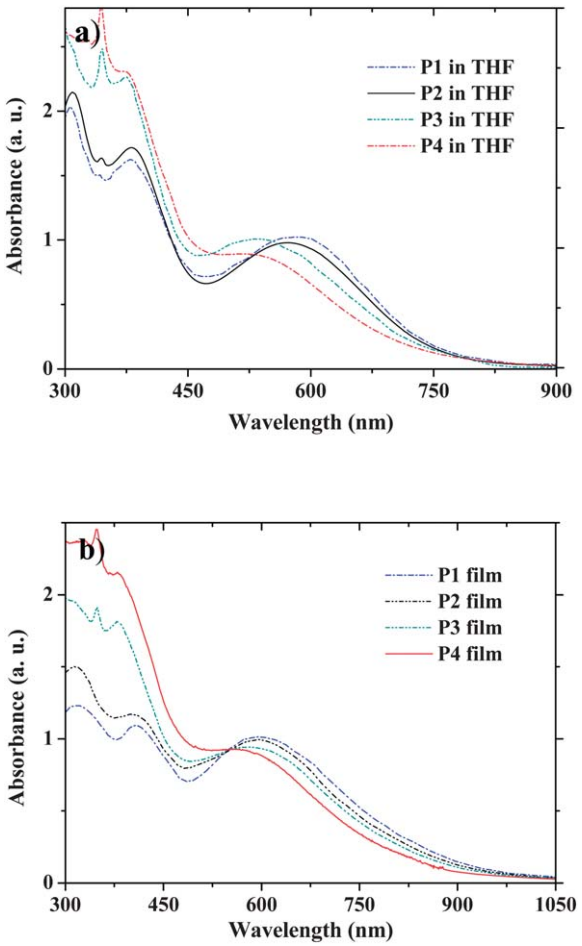

Fig. 1 Optical absorption spectra of **P1–P4** in THF solution (a) and thin film on glass (b).

A similar behavior was observed for the absorption spectra of these copolymers in thin solid films (Fig. 1b). As compared to their counterparts in the solution state, the broad peaks in the wavelength range of 450–1000 nm showed different red-shifts from 7, 16, 29, 34 nm for **P1**, **P2**, **P3** and **P4**, respectively. The reason can be explained by the formation of π-stacked structures in the solid state[30] which could facilitate charge transportation for photovoltaic applications. The level of red-shift obviously relied on the content of cofacial indolo[3,2-*b*]carbazole groups. The energy band gaps calculated from the absorption band edges of the optical absorption spectra were about 1.31, 1.38, 1.47, and 1.51 eV for polymers **P1–P4**, respectively, indicating an effective narrowing in the band gap energy by increasing the PQx content in the polymer backbone.

Electrochemical properties

The redox behavior of the copolymer films on Pt plate electrodes was studied by cyclic voltammetry (CV), which is used to

Table 2 Optical and electrochemical data of the copolymers

Copolymers	Abs. (nm) λ_{max}^{THF}	Abs. (nm) λ_{max}^{film}	E_g[a] (eV)	E (V)/HOMO (eV)	E (V)/LUMO (eV)	E_g[b] (eV)
P1	381, 588	409, 595	1.31	0.62/−5.02	−0.67/−3.73	1.29
P2	378, 574	401, 590	1.38	0.70/−5.10	−0.70/−3.70	1.40
P3	374, 551	383, 580	1.47	0.74/−5.14	−0.76/−3.64	1.50
P4	372, 541	379, 575	1.51	0.75/−5.15	−0.89/−3.51	1.64

[a] Optical band gap was estimated from the wavelength of the optical absorption edge of the copolymer film. [b] Electrochemical band gap was calculated from the LUMO and HOMO energy levels.

determine the energy levels of the highest occupied molecular orbital (HOMO) and the lowest unoccupied molecular orbital (LUMO). The CV measurements were performed using a three-electrode cell in an anhydrous CH_3CN solution of 0.1 M tetrabutylammonium perchlorate (n-Bu_4NClO_4). A Pt wire was used as the counter electrode and Ag/AgCl (0.1 M) as the reference electrode. The energy level of the Ag/AgCl reference electrode (calibrated against the FC/FC^+ redox system) was 4.40 eV below the vacuum level.[33] The cell was purged with pure argon prior to each scan. The scans toward the anodic and cathodic directions were performed separately at a scan rate of 50 mV s^{-1} at room temperature. As shown in Fig. 2, all the copolymers show good reversibility in the n-doping processes due to the electron-rich indolo[3,2-b]carbazole and thiophene units and p-doping processes due to the electron-poor pyrazino[2,3-g]quinoxaline units.

On anodic sweep, the onset potentials of the p-doping process for polymer **P1**, **P2**, **P3** and **P4** are determined to be 0.62, 0.70, 0.74, and 0.75 V, which correspond to a HOMO energy level (E_{HOMO}) of 5.02, 5.10, 5.14 and 5.15 eV, respectively. Obviously, the increase in oxidation potentials of these copolymers can be attributed to the higher content of indolo[3,2-b]carbazole units incorporated into the polymer main chains. On sweeping the polymers cathodically, the onset potentials of the n-doping process for **P1**, **P2**, **P3** and **P4** occur at about −0.67, −0.70, −0.77 and −0.89 V. The lowest unoccupied molecular orbital (LUMO) energy levels of the corresponding copolymers are estimated to be −3.73, −3.70, −3.64 and −3.51 eV, respectively. From the onset potentials of the oxidation and reduction processes, the band gaps (E_g) of the **P1**, **P2**, **P3** and **P4** were calculated to be about 1.31, 1.38,1.47 and 1.51 eV. The values are close to those obtained by the optical method described above. The electrochemical data of the copolymers are summarized in Table 2.

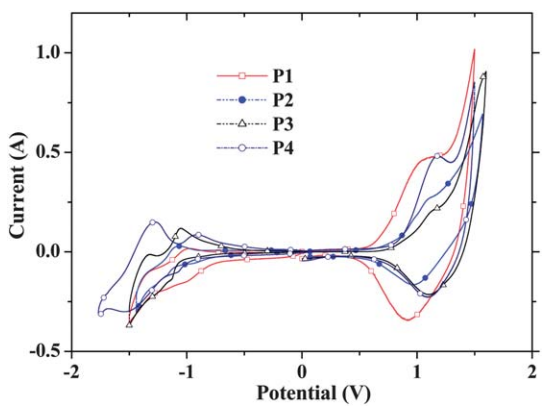

Fig. 2 Cyclic voltammograms of the copolymers **P1–P4**.

Theoretical calculations

DFT/B3LYP/6-31G* has been found to be an accurate method for calculating the optimal geometry and electronic structures of many molecular systems. To gain insight into the nature of the excited states of the copolymers, we performed density functional theory (DFT) calculations at the B3LYP/6-31G* level on a D–A model compounds and optimized their geometrical structures followed by calculation of the lowest vertical excitations using the Gaussian 09 program suite.[34] The alkyl groups were not included in the calculation because they do not significantly affect the equilibrium geometry and the electronic properties.

Fig. S1† shows the molecular structures and molecular orbitals (HOMO and LUMO) of the model compounds. *Ab initio* calculations on the model compounds for the resulting copolymers show that they are planar molecules, which enable the electrons to be delocalized within the molecule systems by conjugation to get higher carrier mobility.[35] As shown in Fig. S1,† the results indicate that the electron density of LUMO is mainly localized on the pyrazino[2,3-g]quinoxaline unit, while the electron density of HOMO is distributed over the entire conjugated molecule. Calculated results show that the D–A model molecules have HOMO energy levels from −4.75 eV to −4.46 eV and a LUMO energy level from −2.98 eV to −3.22 eV. The band gap is determined to be about 1.77 eV to 1.24 eV. Obviously, the HOMO energy levels increase with the content of pyrazino[2,3-g]quinoxaline units, however, the LUMO energy levels and band gaps decrease. The results are in good agreement with those obtained by CV and UV-vis measurements. However, these values from calculations are somewhat difference compared to experimental data due to the part extended π-conjugation system or just several repeat sections chosen from copolymers. Anyway, these calculated values for LUMO, HOMO levels and band gaps of model compounds are still important to predict the trend of experimental results allowing a rapid screening of the most promising polymeric structures.

Photovoltaic properties

As described above, the resulting coplanar copolymers are promising materials for polymer photovoltaic applications. The bulk-heterojunction (BHJ) polymer photovoltaic cells (PVCs) were fabricated using a similar method to our previous work[19,30] with a conventional sandwich structure of ITO/PEDOT:PSS/

active layer/Ca/Al by spin-coating from a chlorobenzene solution of copolymer/PCBM blend as the active layer. The devices were optimized by changing some conditions, such as the ratio of the copolymer and PCBM, the thickness of active layer, the thermal annealing temperature. For this work, using Ca/Al as the cathode and annealing the blend films at 110 °C for 5 min afforded the best device performance. Better fabrication conditions were obtained by spin-coating from a 10 mg mL^{-1} chlorobenzene solution of copolymer/[60]PCBM ratio of 1 : 3 (w/w).

Current–voltage (*I–V*) curves of the PVCs based on **P1–P4** are also shown in Fig. 3a. The open-circuit voltage (V_{oc}), short-circuit current (J_{sc}), fill factor (FF), and power conversion efficiency (PCE) values of these devices under the illumination of AM1.5 (100 mW cm^{-2}) were measured to be 0.70 V, 3.18 mA cm^{-2}, 0.41, and 0.91% for **P1**; 0.79 V, 4.09 mA cm^{-2}, 0.41 and 1.32% for **P2**; 0.83 V, 5.70 mA cm^{-2}, 0.45 and 2.13% for **P3**; and 0.82 V, 5.16 mA cm^{-2}, 0.42, and 1.78% for **P4**, respectively. Table 3 summaries the corresponding data of the devices. Obviously, increasing the content of indolo[3,2-b]carbazole units in the polymer main chains has enhanced the efficiency of PVCs. After the ratio reaching to some extent of 0.7 : 0.3, the carrier mobility may not play a preponderant role compared to the absorption and led to decreased efficiency. Anyway, considering the relatively low FF of these devices (0.41–0.45), there is a plenty room for future improvement in performance of PVCs based on the resulting copolymer/PCBM system.

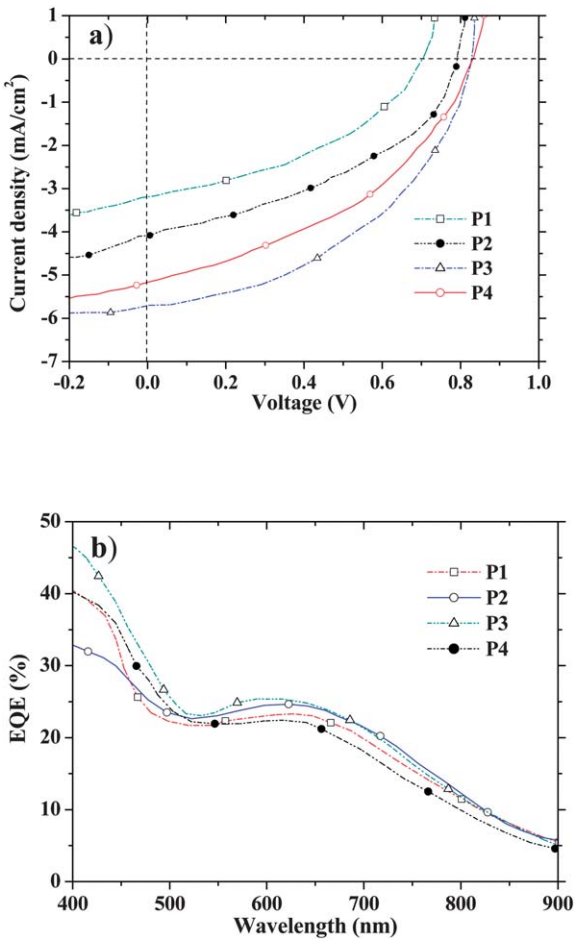

Fig. 3 (a) Current–voltage curves of photovoltaic cells based on copolymers together with [60]PCBM under AM 1.5 illumination, (b) EQE curves of photovoltaic cells based on copolymers together with [60]PCBM.

Fig. 3b shows the external quantum efficiency (EQE) curves of the optimized PVCs with copolymer:[60]PCBM under the illumination of monochromatic light. As shown in Fig. 3b, the shape of the EQE curves is similar to the absorption spectra, indicating that all the absorption wavelengths of the polymers contributed to photocurrent generation. That is to say the excitons are mainly generated in copolymer phases. However, the broader profile and high values of EQE were observed which consistent with the high J_{SC} measured in these PVCs.

[70]PCBM has similar electronic properties as [60]PCBM, but a relatively higher absorption coefficient in the visible region,[36] which can be used to compensate for the poor absorption of copolymer/[60]PCBM blend in the range of 400–500 nm. For the purpose of direct comparison, the copolymer [70]PCBM based PVCs were further fabricated to get better efficiencies instead of [60]PCBM. To understand the role of the **P3**/[70]PCBM blend composition on the photovoltaic properties, PVCs with **P3**:[70]PCBM ratios of 1 : 1, 1 : 2, 1 : 3, and 1 : 4 were fabricated and measured. All the photovoltaic parameters including J_{sc}, V_{oc}, FF, and PCE for these devices are also summarized in Table 3. The *I–V* characteristics of the devices from **P3**/[70]PCBM are described in Fig. 4a. The J_{sc} first increased from 4.66 mA cm^{-2} at a **P3**/[70]PCBM ratio of 1 : 1 to 9.55 mA cm^{-2} at 1 : 1 composition, but decreased to 6.48 mA cm^{-2} at a **P3**/[70]PCBM ratio of 1 : 4. The PVC from **P3**/[70]PCBM =1 : 3 has the highest PCE of 3.24% under the illumination of AM1.5 (100 mW cm^{-2}), with a J_{sc} of 9.55 mA cm^{-2}, an V_{oc} of 0.81 V, and an FF of 0.42. The efficiency increased significantly in comparison with that obtained from [60]PCBM based cells, which was mainly attributed to the enhanced photoresponse in the visible region. As shown in Fig. 4b, it is obvious that the valley in the range of 400–500 nm was efficiently compensated for and gives rise to higher J_{sc}. The enhanced absorption and thus improved light harvesting in the PVCs using [70]PCBM is also consistent with the observed enhanced device efficiency. The V_{oc} in these four devices changed just a little without improvement. Generally, the V_{oc} in polymer/PCBM BHJ solar cells is related to the energy difference between the HOMO energy level of the donor and the LUMO energy level of the acceptor. So the obtained values in this work have almost achieved the limits for the V_{oc}. The FF reflects the fraction of photogenerated charge carriers that reached the electrodes. However, the FFs in this work are not so high. Nevertheless, further work to identify the optimized electrodes and device performance is still ongoing.

Conclusions

A new series of low band gap copolymers based on electron-accepting pyrazino[2,3-g]quinoxaline (PQx) and an coplanar electron-donating indolo[3,2-b]carbazole and thiophene units have been synthesized by Stille coupling polymerization. Their optical and electrical properties can be facilely fine-modulated by adjusting the donor/acceptor ratios. All these copolymers exhibit good light conversion efficiency with low band gaps. UV-vis spectra showed that increasing the number of PQx units led to

Table 3 Characteristic current–voltage parameters from device testing at standard AM 1.5G conditions

Copolymers	copolymer/PCBM (w/w)	V_{OC} (V)	J_{SC} (mA cm^{-2})	FF	PCE (%)
P1	1 : 3[a]	0.70	3.18	0.41	0.91
P2	1 : 3[a]	0.79	4.09	0.41	1.32
P3	1 : 3[a]	0.83	5.70	0.45	2.13
P3	1 : 1[b]	0.78	4.66	0.44	1.60
P3	1 : 2[b]	0.83	6.84	0.44	2.52
P3	1 : 3[b]	0.81	9.55	0.43	3.24
P3	1 : 4[b]	0.80	6.48	0.45	2.36
P4	1 : 3[a]	0.82	5.16	0.42	1.78

[a] Using [60]PCBM as acceptors. [b] Using [70]PCBM as acceptors.

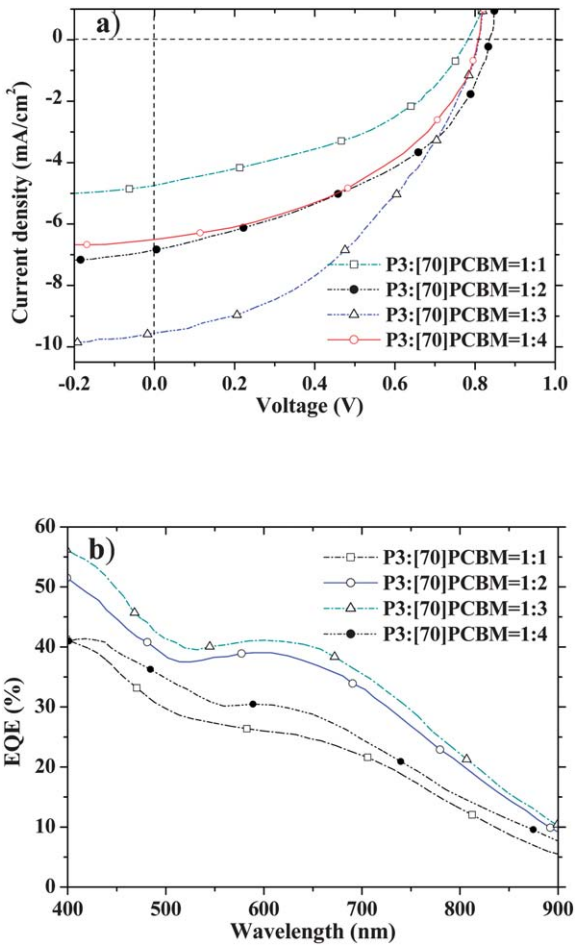

Fig. 4 (a) Current–voltage curves of photovoltaic cells based on copolymer **P3** together with [70]PCBM under AM 1.5 illumination, (b) EQE curves of photovoltaic cells based on copolymer **P3** together with [70]PCBM.

a red-shift in the optical absorption. The band gaps calculated based on UV-vis spectra, CV scanning, and DFT modeling all indicated a narrowing band gap with increasing the PQx content in the copolymer structures. The PSCs based on these copolymers were fabricated with a structure of ITO/PEDOT:PSS/copolymer:PCBM/Ca/Al under the illumination of AM 1.5G, 100 mW cm^{-12}. The results showed that increase the content of indolo[3,2-b]carbazole units in the copolymer chains had enhanced the efficiencies of PVCs. If the ratio reached the value of 0.7 : 0.3, the efficiency would decrease because the carrier mobility does not play a preponderant role compared to the absorption. The best performing copolymer in a device using [70]PCBM as accepters was **P3** with J_{sc} = 9.55 mA cm^{-2}, V_{oc} = 0.81 V, FF = 0.42, and PCE = 3.24%, which is the highest efficiency for the PQx and indolo[3,2-b]carbazole based on PVCs. The present results indicate that the efficient photovoltaic materials with suitable electronic and optical properties can be achieved by just fine-tuning the ratios of the strong electron-deficient accepters and large-π planar donors.

Experimental

Materials and instruments

NMR spectra were recorded on a Bruker Avance-400 spectrometer with *d*-chloroform as the solvent and tetramethylsilane as the internal standard. Cyclic voltammetry measurements were made on an CHI660 potentiostat/galvanostat electrochemical workstation at a scan rate of 50 mV s^{-1}, with a platinum wire counter electrode and a Ag/AgCl reference electrode in an anhydrous and nitrogen-saturated 0.1 mol L^{-1} acetonitrile (CH_3CN) solution of tetrabutylammonium perchlorate (Bu_4NClO_4). The copolymers were coated on the platinum plate working electrodes from dilute chloroform solutions. UV-vis spectra were obtained on a Carry 300 spectrophotometer. Thermogravimetric analysis (TGA) and differential scanning calorimetry (DSC) measurements were conducted on a TA Instrument Model SDT Q600 simultaneous TGA/DSC analyzer at a heating rate of 10 °C min^{-1} and under a N_2 flow rate of 90 mL min^{-1}. Polymer photovoltaic cells were fabricated with ITO glass as an anode, Ca/Al as a cathode, and the blend film of the copolymer and 1-(3-methoxycarbonyl) propyl-1-phenyl-6,6-methanofullerence (PCBM) as a photosensitive layer. The photosensitive layer was prepared by spin-coating a blend solution of the copolymer and PCBM in chlorobenzene on the ITO/PEDOT:PSS electrode. The current–voltage (*I–V*) characterization of the devices was carried out on a computer-controlled Keithley 236 Source Measurement system. A solar simulator was used as the light source, and the light intensity was monitored by a standard Si solar cell. The thickness of films was measured using a Dektak 6 M surface profilometer.

All reagents were purchased from aladdin Co., Alfa Aesar Co. and Aldrich Chemical Co., unless stated otherwise. Commercial chemicals were used without further purification. 4,7-Dibromobenzo[2,1,3]thiadiazole (**1**) and 4,7-dibromo-5,6-dinitro-benzo

[2,1,3]thiadiazole (**2**) were synthesized according to the literature.[37]

4,7-Di(4-hexyl)thiophen-2-yl-5,6-dinitro-benzo[2,1,3]thiadiazole (3). A solution of 4,7-dibromo-5,6-dinitro-benzo[2,1,3]thiadiazole (2) (5.50 g, 14.4 mmol) and 3-hexyl-5-(tribytylstannyl) thiophene (16.03 g, 35.10 mmol) in freshly distilled THF (70 ml) was degassed. The mixture was heated to reflux under a nitrogen atmosphere and then dichlorobis(triphenylphosphine)palladium (II) [$PdCl_2(PPh_3)_2$] (203mg, 0.29 mmol) was added. After 12 h, the THF was removed off by vacuum distillation. The residues were purified by column chromatography (eluant: petroleum ether: $CHCl_3$ = 2 : 1) to give pure compound **3** (6.20 g, 77%) as an orange solid. mp 53–56 °C. ^{1}H NMR ($CDCl_3$, 400 MHz, δ (ppm)): 7.25 (1H, s, thiophene-H), 7.19 (1H, s, thiophene-H), 2.60 (4H, t, α-CH_2), 1.58 (4H, m, CH_2), 1.30–1.18 (12H, m, CH_2), 0.85–0.81 (6H, m, CH_3). ^{13}C NMR ($CDCl_3$, 100 MHz, δ (ppm)): 144.40, 132.17, 129.20, 126.40, 121.42, 31.63, 30.30, 30.25, 28.88, 22.59, 14.07.

2,3,6,7-Tetraethyl-9,10-di(4-hexyl)thien-2-ylpyrazino[2,3-g]quinoxaline (4). A suspension mixture of zinc dust (4.86g, 74.41 mmol) and 4,7-di(4-hexyl)thiophen-2-yl-5,6-dinitro-benzo[2,1,3] thiadiazole (**3**) (2.0 g, 3.58 mmol) in acetic acid (35 ml) was kept at 60 °C for one and a half hours. The reaction mixture turned pale green slowly. The solution was cooled to room temperature and 3,4-hexanedione (2.45 g, 21.48 mmol) was added. The mixture was stirred vigorously for 24 h at room temperature. The solvent and excess 3,4-hexanedione were removed off by vacuum distillation. The residues were purified by column chromatography (eluant: petroleum ether: $CHCl_3$ = 1 : 1) to give pure compound **4** (1.25 g, 56%) as a red solid. mp 102 °C. ^{1}H NMR ($CDCl_3$, 400 MHz, δ (ppm)): 8.26 (2H, s, thiophene-H), 7.16 (2H, s, thiophene-H), 3.10–3.05 (8H, q, α-CH_2), 2.67 (4H, t, α-CH_2), 1.73–1.65 (4H, m, CH_2), 1.51–1.47 (12H, q, CH_3), 1.37–1.26 (12H, m, CH_2), 0.84 (6H, t, CH_3). ^{13}C NMR ($CDCl_3$, 100 MHz, δ (ppm)): 156.35, 141.61, 136.32, 135.41, 134.25, 127.87, 124.35, 31.81, 30.77, 30.70, 29.18, 28.36, 22.64, 14.14, 11.52.

2,3,6,7-Tetraethyl-9,10-di(5-dibromo-4-hexyl)thien-2-ylpyrazino[2,3-g]quinoxaline (5). To a solution of 2,3,6,7-tetraethyl-9,10-di(4-hexyl)thien-2-ylpyrazino[2,3-g] quinoxaline (**4**) (1.60 g, 2.55 mmol) in chloroform (60 ml) and of acetic acid (25 ml), N-bromosuccimide (NBS) (1.82 g, 10.20 mmol) was added. This mixture was then stirred for 4 h at room temperature in darkness. The solvent was removed off by vacuum distillation. The residues were purified by column chromatography (eluant: petroleum ether: $CHCl_3$ = 2 : 1) to give pure compound **5** (2.57 g, 79%) as a red solid. mp 118 °C. ^{1}H NMR ($CDCl_3$, 400 MHz, δ (ppm)): 8.54 (1H, s, thiophene-H), 8.45 (1H, s, thiophene-H), 3.14–2.91 (8H, m, α-CH_2), 2.73–2.60 (4H, m, α-CH_2), 1.66–1.60 (4H, m, CH_2), 1.53–1.49 (8H, q, CH_2), 1.37–1.26 (16H, m, CH_2, CH_3), 0.87–0.82 (6H, q, CH_3). ^{13}C NMR ($CDCl_3$, 100 MHz, δ (ppm)): 157.29, 140.29, 133.96, 135.75, 134.52, 129.28, 126.56, 31.74, 30.30, 29.86, 28.90, 28.36, 22.60, 14.12, 11.89.

3,9-dibromo-11-hexyl-indolo[3,2-b]carbazole (6). To a solution of 5-bromoindole (7.25 g, 37 mmol) and *n*-heptaldehyde (2.06 g, 18 mmol) in acetonitrile (50 ml), a few drops of HI was added by dropwise as catalyst. The reaction mixture was stirred for 14 h at room temperature under a nitrogen atmosphere. After that, the excess saturated sodium sulfite solution was added into the mixture and extracted with ethyl acetate. The filtrate was dried with anhydrous magnesium sulfate and the solvent was removed off by vacuum distillation to afford intermediate compound. The crude product was dissolved in a mixture of triethyl orthoformate (2.67 g, 18 mmol), methanesulfonic acid (0.36 g, 3.7 mmol) and methanol (20 ml) without purification. The solution was stirred overnight at room temperature. The precipitates were filtered and washed with methanol to give a yellow solid **6** (1.64 g, 17.8%). mp 223 °C. ^{1}H NMR ($CDCl_3$, 400MHz, δ (ppm)): 11.39 (1H, s, N–H), 11.19 (1H, s, N–H), 8.46 (1H, s, Ph-H), 8.20 (1H, s, Ph-H), 8.08 (1H, s, Ph-H), 7.54–7.50 (2H, m, Ph-H), 7.47–7.45 (2H, m, Ph-H), 3.46–3.37 (2H, m, α-CH_2), 1.79–1.76 (2H, m, CH_2), 1.62–1.57 (2H, m, CH_2), 1.42–1.31 (4H, m, CH_2), 0.91–0.87 (3H, t, CH_3). ^{13}C NMR ($CDCl_3$, 100 MHz, δ (ppm)): 140.46, 136.51, 134.91, 128.43, 127.76, 125.14, 124.64, 123.47, 122.37, 120.09, 31.65, 29.39, 29.07, 28.62, 22.54, 14.36.

3,9-Dibromo-5, 6,11-trihexyl-indolo[3,2-b]carbazole (7). To a solution of 3,9-dibromo-11-hexyl-indolo[3,2-b]carbazole (**6**) (0.36 g, 0.72 mmol) in DMF (6 ml), NaH (0.048 g, 1.99 mmol) was added slowly. The reaction solution was stirred for 30 minutes and 1-bromohexane (0.36 g, 2.17 mmol) was added by syringe. The mixture was stirred vigorously for 36 h and poured into excess water. The mixture was then extracted with $CHCl_3$ and the organic phase was dried and concentrated to give a yellow solid **7** (0.38 g, 78.9%). mp 171 °C. ^{1}H NMR ($CDCl_3$, 400 MHz, δ (ppm)): 8.25–8.20 (2H, d, Ph-H), 7.74 (1H, s, Ph-H), 7.49 (2H, t, Ph-H), 7.24–7.21 (2H, d, Ph-H), 4.38–4.27 (4H, m, N-CH_2), 3.51 (2H, s, α- CH_2), 1.86–1.77 (6H, m, CH_2), 1.65 (2H, s, CH_2), 1.45–1.22 (16H, m, CH_2), 0.96–0.79 (9H, m, CH_3). ^{13}C NMR ($CDCl_3$, 100 MHz, δ (ppm)): 140.95, 136.56, 133.78, 128.56, 127.60, 125.36, 124.57, 123.49, 122.58, 120.85, 45.88, 43.19, 31.71, 31.60, 30.21, 29.76, 28.79, 28.57, 27.02, 26.70, 22.63, 14.05.

Copolymers. In a typical experiment, 1.0 mmol of the compound **5** and **7** mixture was put into a 100 mL three-necked flask. The feed ratio for each of the components in the mixture was controlled at different values for the preparation of different copolymers (*vide infra*). To the mixture solution, 20 mL of degassed toluene was added under the protection of argon, followed by flushing the solution with argon for 10 min. A total of 50 mg of $Pd(PPh_3)_4$ and 1.0 mmol of 2,5-bis(tributylstannyl) thiophene were then added into the mixture solution. After another flushing with argon for 20 min, the reactant mixture was heated and refluxed for 24 h. 79 μL 2-tributylstannyl thiophene was added to the reaction and then after two hours, 25 μL 2-bromothiophene was added. The mixture was stirred overnight to complete the end-capping reaction. Thereafter, the reaction solution was cooled to room temperature and precipitated by the addition of 500 mL of methanol. The crude copolymer was filtered and extracted in a Soxhlet apparatus with methanol, hexane, and acetone. Finally, the polymer was extracted with chloroform. The polymer solution was condensed to about 20 mL and slowly poured in 500 mL methanol. The solid was filtered and a dark purple solid was obtained with a yield of 69–72%.

P1: Compound **5** (0.7063 g, 0.9 mmol), compound **7** (0.0667 g, 0.1 mmol), 2,5-bis(tributylstannyl)thiophene (0.6622 g, 1.0 mmol), toluene (20 mL), and $Pd(PPh_3)_4$ (50 mg, 0.043 mmol) were used, and the general procedure described previously for the copolymer syntheses was followed (*cf.* Scheme 1). The obtained solid was a dark purple powder with a yield of 68%. $M_n = 7600$, $M_w/M_n = 1.85$. ^1H NMR ($CDCl_3$, 400 MHz, δ (ppm)): 8.60–8.46 (m, thiophene-H), 8.33–8.28 (m, Ph-H), 7.80–7.78 (m, Ph-H), 7.58–7.41 (m, thiophene-H), 7.33–7.23 (m, Ph-H), 4.767–4.23 (m, N-CH_2), 3.43–2.91 (m, α-CH_2), 1.78–1.18 (m, CH_2, CH_3), 0.90–0.82 (m, CH_3). Anal. calcd for $(C_{41.8}H_{49.8}S_{2.8}N_{3.8})x$ C, 72.21; H, 7.22; N, 7.66; S, 12.91. Found: C, 72.34; H, 7.18; N, 7.62; S, 12.98.

P2: Compound **5** (0.6278 g, 0.8 mmol), compound **7** (0.1333 g, 0.2 mmol), 2,5-bis(tributylstannyl)thiophene (0.6622 g, 1.0 mmol), toluene (20 mL), and $Pd(PPh_3)_4$ (50 mg, 0.043 mmol) were used, and the general procedure described previously for the copolymer syntheses was followed (*cf.* Scheme 1). The obtained solid was a dark purple powder with a yield of 70%. $M_n = 8000$, $M_w/M_n = 1.92$. ^1H NMR ($CDCl_3$, 400MHz, δ (ppm)): 8.61–8.55 (m, thiophene-H), 8.38–8.29 (m, Ph-H), 7.81–7.78 (m, Ph-H), 7.61–7.42 (m, thiophene-H), 7.34–7.26 (m, Ph-H), 4.52−4.20 (m, N-CH_2), 3.45–2.91 (m, α-CH_2), 1.80–1.19 (m, CH_2, CH_3), 0.88–0.84 (m, CH_3). Anal. calcd for $(C_{41.6}H_{49.6}S_{3.6}N_{2.6})x$ C, 73.11; H, 7.31; N, 7.38; S, 12.20. Found: C, 73.35; H, 7.26; N, 7.35; S, 12.34.

P3: Compound **5** (0.5493g, 0.7 mmol), compound **7** (0.2000g, 0.3 mmol), 2,5-bis(tributylstannyl)thiophene (0.6622 g, 1.0 mmol), toluene (20 mL), and $Pd(PPh_3)_4$ (50 mg, 0.043 mmol) were used, and the general procedure described previously for the copolymer syntheses was followed (*cf.* Scheme 1). The obtained solid was a dark purple powder with a yield of 72%. $M_n = 8500$, $M_w/M_n = 1.98$. ^1H NMR ($CDCl_3$, 400 MHz, δ (ppm)): 8.63–8.56 (m, thiophene-H), 8.26–8.20 (m, Ph-H), 7.78–7.74 (m, Ph-H), 7.59–7.44 (m, thiophene-H), 7.36–7.23 (m, Ph-H), 4.32–4.26 (m, N-CH_2), 3.49–2.96 (m, α-CH_2), 1.78–1.18 (m, CH_2, CH_3), 0.91–0.81 (m, CH_3). Anal. calcd for $(C_{41.4}H_{49.4}S_{3.4}N_{2.4})x$ C, 74.04; H, 7.41; N, 7.09; S, 11.46. Found: C, 74.28; H, 7.35; N, 7.01; S, 11.51.

P4: Compound **5** (0.4709 g, 0.6 mmol), compound **7** (0.2666 g, 0.4 mmol), 2,5-bis(tributylstannyl)thiophene (0.6622 g, 1.0 mmol), toluene (20 mL), and $Pd(PPh_3)_4$ (50 mg, 0.043 mmol) were used, and the general procedure described previously for the copolymer syntheses was followed (*cf.* Scheme 1). The obtained solid was a dark purple powder with a yield of 69%. $M_n = 7900$, $M_w/M_n = 1.86$. ^1H NMR ($CDCl_3$, 400 MHz, δ (ppm)): 8.63–8.56 (m, thiophene-H), 8.23–8.20 (m, Ph-H), 7.76–7.72 (m, Ph-H), 7.58–7.44 (m, thiophene-H), 7.33–7.22 (m, Ph-H), 4.37–4.23 (m, N-CH_2), 3.46–2.95 (m, α-CH_2), 1.78–1.18 (m, CH_2, CH_3), 0.89–0.84 (m, CH_3). Anal. calcd for $(C_{41.2}H_{49.2}S_{3.2}N_{2.2})x$ C, 75.00; H, 7.52; N, 6.79; S, 10.69. Found: C, 75.32; H, 7.46; N, 6.74; S, 10.73.

Acknowledgements

The work was financially supported by the Natural Science Foundation of China (NSFC, No: 20802033), Program for New Century Excellent Talents in University (No: NCET-10-0170), Yong Scientist of Jing Gang Zhi Xing Project of Jiangxi Province (No: 2008DQ00700), Aviation Science Fund of China (No: 2008ZF56014) and Natural Science Foundation of Jiangxi Province (Grant No: 2010GZH0110).

References

1 S. Günes, H. Neugebauer and N. S. Sariciftci, *Chem. Rev.*, 2007, **107**, 1324.
2 B. C. Thompson and J. M. J. Fréchet, *Angew. Chem., Int. Ed.*, 2008, **47**, 58.
3 J. Y. Kim, K. Lee, N. E. Coates, D. Moses, T. Q. Nguyen, M. Dante and A. J. Heeger, *Science*, 2007, **317**, 222.
4 F. C. Krebs, S. A. Gevorgyan and J. Alstrup, *J. Mater. Chem.*, 2009, **19**, 5442.
5 F. C. Krebs, J. Fyenbo and M. Jørgensen, *J. Mater. Chem.*, 2010, **20**, 8994.
6 C. J. Brabec, S. E. Shaheen, C. Winder, N. S. Sariciftci and P. Denk, *Appl. Phys. Lett.*, 2002, **80**, 1288.
7 G. Li, V. Shrotriya, Y. Yao and Y. J. Yang, *Appl. Phys. Lett.*, 2005, **98**, 437041.
8 F. Padinger, R. S. Rittberger and N. S. Sariciftci, *Adv. Funct. Mater.*, 2003, **13**, 85.
9 W. L. Ma, C. Y. Yang, X. Gong, K. Lee and A. J. Heeger, *Adv. Funct. Mater.*, 2005, **15**, 1617.
10 H. Y. Chen, J. H. Hou, S. P. Zhang, Y. Y. Liang, G. W. Yang and Y. Yang, *Nat. Photonics*, 2009, **3**, 649.
11 Y. Y. Liang, Z. Xu, J. B. Xia, S. T. Tsai, Y. Wu, G. Li, C. Ray and L. P. Yu, *Adv. Mater.*, 2010, **22**, E135.
12 K. L. Mutolo, E. I. Mayo, B. P. Rand, S. R. Forrest and M. E. Thompson, *J. Am. Chem. Soc.*, 2006, **128**, 8108.
13 A. Gadisa, M. Svensson, M. R. Andersson and O. Inganäs, *Appl. Phys. Lett.*, 2004, **84**, 1609.
14 S. H. Chan, C. P. Chen, T. C. Chao, C. Ting, C. S. Lin and B. T. Ko, *Macromolecules*, 2008, **41**, 5519.
15 T. Yamamoto, Z. H. Zhou, T. Kanbara, M. Shimura, K. Kizu, T. Maruyama, Y. Nakamura, T. Fukuda, B. L. Lee, N. Ooba, S. Tomaru, T. Kurihara, T. Kaino, K. Kubota and S. Sasaki, *J. Am. Chem. Soc.*, 1996, **118**, 10389.
16 A. Gadisa, W. Mammo, L. M. Andersson, S. Admassie, F. L. Zhang, M. R. Andersson and O. Inganäs, *Adv. Funct. Mater.*, 2007, **17**, 3836.
17 L. J. Huo, Z. A. Tan, X. Wang, Y. Zhou, M. F. Han and Y. F. Li, *J. Polym. Sci., Part A: Polym. Chem.*, 2008, **46**, 4038.
18 M. H. Lai, C. C. Chuen, W. C. Chen, J. L. Wu and F. C. Chen, *J. Polym. Sci., Part A: Polym. Chem.*, 2009, **47**, 973–985.
19 Q. Peng, J. Xu and W. X. Zheng, *J. Polym. Sci., Part A: Polym. Chem.*, 2009, **47**, 3399.
20 D. Kitazawa, N. Watanabe, S. Yamamoto and J. Tsukamoto, *Appl. Phys. Lett.*, 2009, **95**, 053701.
21 F. L. Zhang, J. Bijleveld, E. Perzon, K. Tvingstedt, S. Barrau, O. Inganäs and M. R. Andersson, *J. Mater. Chem.*, 2008, **18**, 5468.
22 M. Mastalerz, V. Fischer, C. Q. Ma, R. A. J. Janssen and P. Bäuerle, *Org. Lett.*, 2009, **11**, 4500.
23 M. Manceau, E. Bundgaard, J. E. Carlé, O. Hagemann, M. Helgesen, R. Søndergaard, M. Jørgensen and F. C. Krebs, *J. Mater. Chem.*, 2011, **21**, 4132.
24 M. Jørgensen, K. Norrman and F. C. Krebs, *Sol. Energy Mater. Sol. Cells*, 2008, **92**, 686.
25 Y. Li, Y. Wu, S. Gardner and B. S. Ong, *Adv. Mater.*, 2005, **17**, 849.
26 P. L. T. Boudreault, S. Wakim, N. Blouin, M. Simard, C. Tessier, Y. Tao and M. Leclerc, *J. Am. Chem. Soc.*, 2007, **129**, 9125.
27 C. P. Chen, S. H. Chan, T. C. Chao, C. Ting and B. T. Ko, *J. Am. Chem. Soc.*, 2008, **130**, 12828.
28 J. P. Lu, F. S. Liang, N. Drolet, J. F. Ding, Y. Tao and R. Movileanua, *Chem. Commun.*, 2008, 5315.
29 E. J. Zhou, S. P. Yamakawa, Y. Zhang, K. Tajima, C. Yanga and K. Hashimoto, *J. Mater. Chem.*, 2009, **19**, 7730.
30 Q. Peng, K. Park, T. Lin, M. Durstock and L. M. Dai, *J. Phys. Chem. B*, 2008, **112**, 2801.
31 T. Uno, K. Takagi and M. Tomoeda, *Chem. Pharm. Bull.*, 1980, **28**, 1909.
32 B. P. Bandgar and K. A. Shaikh, *Tetrahedron Lett.*, 2003, **44**, 1959.
33 Y. F. Li, Y. Cao, J. Gao, D. L. Wang, G. Yu and A. J. Heeger, *Synth. Met.*, 1999, **99**, 243.

34 M. J. Frisch, G. W. Trucks, H. B. Schlegel, G. E. Scuseria, M. A. Robb, J. R. Cheeseman, G. Scalmani, V. Barone, B. Mennucci, G. A. Petersson, H. Nakatsuji, M. Caricato, X. Li, H. P. Hratchian, A. F. Izmaylov, J. Bloino, G. Zheng, J. L. Sonnenberg, M. Hada, M. Ehara, K. Toyota, R. Fukuda, J. Hasegawa, M. Ishida, T. Nakajima, Y. Honda, O. Kitao, H. Nakai, T. Vreven, J. A. Montgomery, Jr., J. E. Peralta, F. Ogliaro, M. Bearpark, J. J. Heyd, E. Brothers, K. N. Kudin, V. N. Staroverov, R. Kobayashi, J. Normand, K. Raghavachari, A. Rendell, J. C. Burant, S. S. Iyengar, J. Tomasi, M. Cossi, N. Rega, J. M. Millam, M. Klene, J. E. Knox, J. B. Cross, V. Bakken, C. Adamo, J. Jaramillo, R. Gomperts, R. E. Stratmann, O. Yazyev, A. J. Austin, R. Cammi, C. Pomelli, J. Ochterski, R. L. Martin, K. Morokuma, V. G. Zakrzewski, G. A. Voth, P. Salvador, J. J. Dannenberg, S. Dapprich, A. D. Daniels, O. Farkas, J. B. Foresman, J. V. Ortiz, J. Cioslowski and D. J. Fox, *GAUSSIAN 09 (Revision A.2)*, Gaussian, Inc., Wallingford, CT, 2009.
35 S. Cho, J. H. Seo, S. H. Kim, S. Song, Y. Jin, K. Lee, H. Suh and A. J. Heeger, *Appl. Phys. Lett.*, 2008, **93**, 263301.
36 M. M. Wienk, J. M. Kroon, W. J. H. Verhees, J. Knol, J. C. Hummelen, P. A. van Hal and R. A. J. Janssen, *Angew. Chem., Int. Ed.*, 2003, **42**, 3371.
37 E. Perzon, X. J. Wang, S. Admassie, O. Inganäs and M. R. Andersson, *Polymer*, 2006, **47**, 4261.

